

Parametric Modelling of Phase-Shifted Full-Bridge Zero Voltage Switching DC-DC Converter

Oladimeji Ibrahim^{1*}, Nor Zaihar B. Yahaya², Nordin Saad³,
Khairul Nisak Binti Md Hasan⁴, Nahla M. Shannan⁵, Olayinka Sikiru Zakariyya⁶,
Abdulrahman Okino Otuoze⁷

^{1,6,7} Department of Electrical and Electronics Engineering, University of Ilorin, Ilorin, Nigeria

E-mail: ibrahim.o@unilorin.edu.ng

^{2,3,4} Department of Electrical and Electronics Engineering, Universiti Teknologi PETRONAS, Bandar Seri Iskandar, Perak, Malaysia

⁵ Department of Control Engineering, Alnelain University, Khartoum, Sudan

Received: October 02, 2020

Revised: December 12, 2020

Accepted: December 19, 2020

Abstract—Modelling of switching pulse width modulated phase-shifted full-bridge zero voltage converter is highly challenging due to several transitional stages involved in a complete switching cycle. The circuit averaging technique has been favored in the past three decades considering phase-shifted full-bridge converter as a buck-derived converter. This modelling approach requires several assumptions that include zero equivalent series resistance of output capacitor, zero leakage inductance and unity transformer turn ratio which results in a less accurate system dynamics. In this paper, a system identification approach is proposed for obtaining a more accurate model of phase-shifted full-bridge PWM switching converter using the input-output test data. The model parameter estimation is implemented in Simulink environment incorporating all circuit parasitic parameters and the resulting system's frequency response shows a good agreement when compared with reported measured response.

Keywords— System identification; Full-bridge converter; Zero voltage switching; Transfer function; Recursive least square.

1. INTRODUCTION

The dynamic model of a system is an important prerequisite for effective model-based controller design. It enables design engineers to predict system stability merging and transient response to perturbation. The model of a system can be obtained from mathematical relations using the first principle or from experimental data using system identification techniques [1, 2]. System modelling from the first principle approach requires some level of assumption to avoid complex relation if all system variables are to be considered in a multiphase system. On the other hand, the system identification process involves the use of system measured data to determine or estimate the dynamic model. The later approach offers a simplified alternative approach for constructing or estimating a system model. The system identification technique found its application in adaptive or predictive control of nonlinear systems, fault detection, online and offline model of complex process and time-variant systems such as switching mode power converters [3, 4].

Switch-mode power converters exhibit time-variant dynamics due to the non-linear behaviour of switching element that constitutes a major component of the system. As reported in several literatures, the linear continuous time-invariant model has been widely used to represent switching mode power converter dynamics owing to the simplicity of analysis [1, 2]. The two common approaches for small-signal analysis of pulse width

* Corresponding author

modulation (PWM) converter are the circuit averaging technique and state-space averaging technique (SSA) [5-8]. Several switched mode power converter topologies are used for power conversion in renewable energy systems' applications, but the advantage of high power handling capability makes the zero voltage switching full bridge DC-DC converter topology most suitable for high-power applications [9, 10]. Considering the stages involved in a complete switching cycle of phase-shifted (PS) full-bridge (FB) zero-voltage switching (ZVS) DC-DC converter, it is difficult to derive a meaningful model with state-space averaging technique and this makes the circuit averaging technique a better choice and most widely used method. The averaged circuit model of PS-FB ZVS converter was first proposed by Vlatkovic et al. [11] and it has since been widely adopted by many authors. Recently, an enhanced model with less number of assumptions was presented in [12] with special consideration for system parasitic to account for losses in the system. A transient and small signal analysis of zero-voltage-switched phase-controlled PWM converter based on averaged switched circuit was proposed in [13]. The model derivation was based on the three-terminal averaged PWM switched model developed by Vorpérian [14] with some assumption on parasitic circuit elements. Schutten et al. also proposed a closed-form cycle-by-cycle analysis of ZVS PS-FB converter's small-signal model based on unconventional averaging technique using discretely sampled data [15]. The laborious mathematical derivation involved makes the analysis a bit complex and the resulting model is considered to have equivalent results as the most available simplified models.

Obtaining zero voltage switching PS-FB DC-DC converter model from the first principle involves several assumptions and the resulting model does not always represent the true system dynamics. The system identification technique is considered a better alternative approach to model PWM converter with proper account for circuit parasitic effect on the system behaviour. The switching power converters are generally characteristics with nonlinear behaviour due to the presences of switches such as MOSFETs, IGBTs and transistors with inherent parasitic that affects the system dynamics under different switching and loading conditions [16]. Obtaining the system's model using averaging or state space techniques from the small signal analysis cannot account for the system total dynamics over the operational condition of load changes. The system identification approach allows for a more accurate model where all the components parasitic parameters are easily modelled into the system prior to data collection for the system model estimation. The resulting accurate model will ensure improved system dynamic performance and also aid proper controller design for good system stability to a wide input range and rapid load changes during operation.

The system identification process involves the use of system input-output measured data to determine the system dynamic model. The major part of system identification process is the model parameter estimation. Several adaptations and filtering algorithms have been developed for system model parameter estimate including the popular least square means (LSM), normalized least-square means (NLSM), and the recursive least square (RLS) algorithm [17-22]. These algorithms have been widely applied for both offline and online parameter estimation of DC-DC converters for designing fixed and adaptive gain controller design to achieve tight output voltage regulation [23, 24]. Among these adaptive filter algorithm, the RLS is considered as one of the most widely used methods in system

identification and signal processing due to fast convergence rate and good accuracy [25, 26]. The RLS - like other adaptive filtering algorithms- computes the model parameter through iterative process that repeatedly finds coefficients that minimize the quadratic cost function of the predicted model error. The RLS adaptation algorithm employs batch process based on least square (LS) algorithm which ensures that the sum of the squares of the difference between the actual and the computed values multiply by a cost function is minimal [27].

In this work, system identification approach is used to estimate the model parameters of a PS-FB ZVS DC-DC converter. A 3 kW DC-DC converter is designed and modelled in MATLAB/Simulink environment for obtaining the system input-output voltage data. The obtained data is in turn used to estimate the parameters of different selected model structure based on the RLS algorithm. The use of RLS algorithm for the model parameter estimation offers an easy approach for obtaining a more accurate model of the system with no circuit parasitic assumption since all parasitic elements are part of the built system for data collection. The resulting model captures the effect of the parasitic elements on the system dynamics which is prerequisite for effective controller design for the converter closed-loop voltage regulation to line-load changes.

2. PHASE SHIFTED FULL-BRIDGE DC-DC CONVERTER MODELLING

A PS FB PWM DC-DC converter is an isolated converter, widely used in high voltage, high power applications. It is a buck-derived converter consisting of H-bridge two pair switching legs, isolated transformer, secondary rectifier, and output low pass filter. Fig. 1(a) shows the topology of the FB converter and Fig. 1(b) shows the waveforms of each of the basic transformer primary voltage V_{AB} , primary current I_p , and the secondary voltage V_s . The detail steady-state analysis, design and the circuit operation has been presented in [28, 29]. The steady-state circuit analysis of the DC-DC converter shows that the duty cycle modulation depends on the secondary transformer voltage, primary duty cycle, leakage inductance, output filter inductor current, input voltage, and the switching frequency.

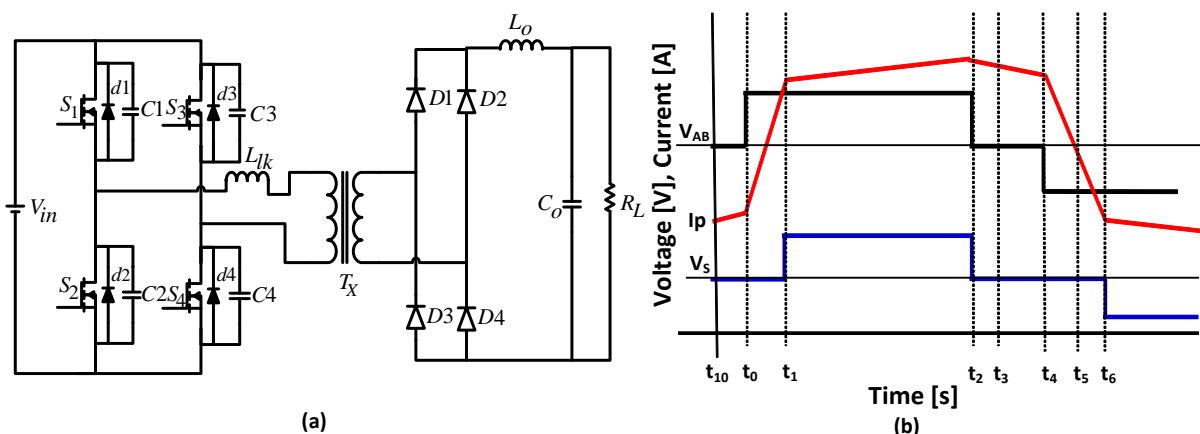


Fig. 1. a) FB converter topology; b) ZVS PS-FB converter waveform.

2.1. System Identification

System identification process involves data gathering, model estimation after the selection of model structure and model validation with independent data [30, 31]. In this

investigation, the PS-FB DC-DC converter small signal model was obtained through parametric identification from the acquired system input-output data. The process starts with the collection of sets of input-output voltage data of the converter as implemented in the MATLAB/Simulink environment. The data were then used to estimate the plant control-to-output transfer function and the frequency response shows good agreement with that of a recently published measured response. The block diagram in Fig. 2 shows the system identification process with the plant (unknown system) and model structure having the same voltage signal input $u(t)$ and the resulting error is minimized by RLS adaptive filter. The main objective of the tuning algorithm is to ensure that the unknown system output is close to the model output as much as possible. If there is high disparity, the model parameters are continually updated until the best fit for the model structure is obtained. Having a high percentage model fit for a specified model structure might not necessarily represent the best fit but increases the ability of the model to repeat the degree of fitness after a series of tests with independent data sets.

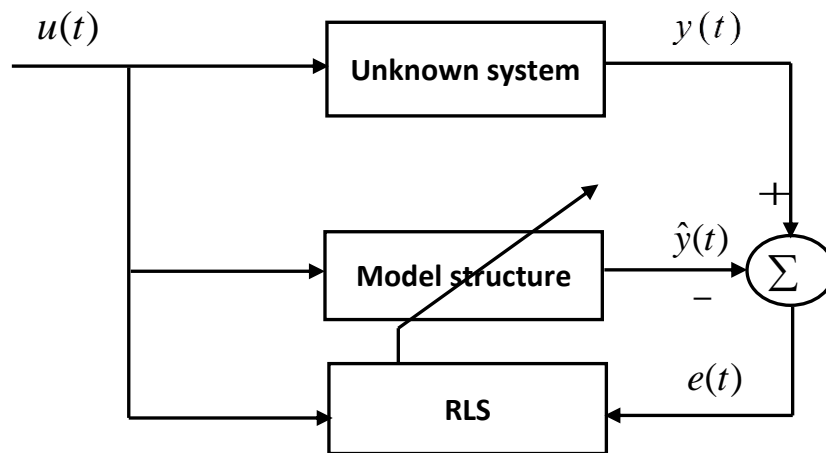


Fig. 2. Block diagram of the system identification process.

The RLS is considered as one of the most widely used adaptive algorithms in system identification and signal processing due to the advantages of fast convergence rate and high estimation accuracy [25]. Although the RLS algorithm has fast convergence rate, there is an issue on high computation complexity due to matrix inversion involvement and hence different methods have been proposed to reduce the computational complexity such as matrix inversion lemma. The unknown model parameter is determined by the least square algorithm that recursively finds the weighting factor that minimizes the prediction error of the quadratic function. The following equations summarise the RLS algorithm for the model parameter estimation.

The RLS algorithm estimates systems using the batch process that depends on the LS estimation. The objective of LS is to ensure that sum of the squares of the differences (error) between the actual (observed) values and the computed value (model) multiplied by a function is minimal. For a given linear system, the observed parameter $y(t)$ can be expressed as:

$$y(t) = \varphi_1 \mathcal{G}_1 + \varphi_2 \mathcal{G}_2 + \dots + \varphi_n \mathcal{G}_n \quad (1)$$

where $\varphi_1, \dots, \varphi_n$ are known functions and $\mathcal{G}_1, \dots, \mathcal{G}_n$ are the actual model parameters.

Eq. (1) can be expressed in vectoral form as:

$$y(i) = \underline{\varphi}^T(i)\mathcal{G} \quad (2)$$

The LS objective is to estimate the unknown parameter θ such that the computed output $\hat{y}(i) = \underline{\varphi}^T(i)\mathcal{G}$ is close to the observed output $y(i)$ in the least square sense, such that the following cost function $J(\theta, t)$ is minimized

$$J(\theta, t) = \sum_{i=1}^t [y(i) - \underline{\varphi}^T(i)\mathcal{G}]^2 \quad (3)$$

in order to obtain the minimum value, $\frac{\partial J(\theta, t)}{\partial \underline{\theta}} = 0$

The LS estimated parameter is obtained as:

$$\hat{\underline{\theta}} = \underline{\theta} = \left[\sum_{i=1}^t \underline{\varphi}(i)\underline{\varphi}^T(i) \right]^{-1} \left[\sum_{i=1}^t \underline{\varphi}(i)y(i) \right] \quad (4)$$

$$\text{If } P(t) = \left[\sum_{i=1}^t \underline{\varphi}(i)\underline{\varphi}^T(i) \right]^{-1}$$

$$\text{Then, } \hat{\underline{\theta}}(t) = P(t) \sum_{i=1}^t \underline{\varphi}(i)y(i)$$

and, the LS estimated parameter solution is given by:

$$\hat{\underline{\theta}}(t) = \hat{\underline{\theta}}(t-1) + P(t)\underline{\varphi}(t)[y(t) - \underline{\varphi}^T(t)\hat{\underline{\theta}}(t-1)] \quad (5)$$

From Eq. (5), the estimated parameter $\hat{\underline{\theta}}(t)$ depends on the previous estimated $\hat{\underline{\theta}}(t-1)$ plus the correction term $P(t)\underline{\varphi}(t)[y(t) - \underline{\varphi}^T(t)\hat{\underline{\theta}}(t-1)]$. The $P(t)\underline{\varphi}(t)$ is the estimator gain $k(t)$ that determines how the current prediction error affects the update of the parameter estimate and the term $y(t) - \underline{\varphi}^T(t)\hat{\underline{\theta}}(t-1)$ is the prediction error $\varepsilon(t)$.

2.2. Converter Model Parameter Estimation

A 3 kW PS-FB ZVS DC-DC converter was designed and modelled in Simulink environment to test data collection. The converter was designed for 40% zero-voltage switching range and the waveform is first investigated to confirm the operational suitability of the converter for model data collection. The Simulink model of the converter incorporated circuit parasitic to cater for losses during circuit operation. The MOSFET *on*-resistance (R_{on}), inductor internal resistance (r_L), capacitance equivalent resistance (ESR_o), and real transformer turn ratio are all modelled as part of the system based on the design specifications provided in Table 1. The steady-state parameters and design calculations are detailed in [29].

The input-output voltage measurement of the converter is used to obtain the dynamic model through the system identification approach. Arbitrary voltage within the designed supply voltage range of 36V~ 60V under full load condition was provided to the system and the corresponding output voltage were recorded. Following the acquisition of the converter input-output operational voltages, the model structure is selected for parameters estimation based on the RLS algorithm as described in subsection 2.1.

Table 1. Converter specifications.

Parameter	Value
Nominal input voltage (V_{in})	48 V
Source voltage range	(36~60) V
Output voltage (V_o)	400 V
Load voltage ripple (V_r)	1 V
Load current (I_o)	7.5 A
Load current ripple	1.5 A
Switching frequency (f_s)	100 kHz
Load resistance (R_L)	53.33 Ω
MOSFET <i>on</i> -resistance (R_{on})	37 m Ω
Capacitance equivalent resistance (r_C)	20 m Ω
Inductor internal resistance (r_L)	10 m Ω
Transformer turn ratio (n)	1:14

A general representation of linear time-invariant transfer function is presented in Eq. (6). The selection of model structure in this work was informed by the earlier presented enhanced model transfer function in which the converter model is second order with 1-zero arising from the equivalent series resistance (ESR_o) of the output filter capacitor [12]. The consistency and suitability of the model structure is verified by testing for higher-order structure up to fourth-order and by using other independent input-output open-loop test data of the converter.

$$\frac{\hat{Y}(s)}{U(s)} = \frac{b_o s^n + b_1 s^{n-1} + \dots + b_{n-1} s + b_n}{s^n + a_1 s^{n-1} + \dots + a_{n-1} s + a_n} \quad (6)$$

The converter model parameters' estimation was carried out in MATLAB/Simulink environment using *system Identification toolbox*. The open-loop test data was imported to the tool-box and pre-processed by detrending the data offset before the RLS algorithm is used to estimate the system transfer function. The parameters estimation is carried out for four different models' structures using same plant data; **tf1** (1-pole, no-zeros), **tf2** (1-pole, 1-zero), **tf3** (2-poles, 1-zeros), **tf4** (3-poles, 1-zero) and were found to have 96.57%, 98.55%, 99%, 98.56% best fits, respectively as presented in the results section. The obtained model is validated with two other independent data sets before analysing it in both time and frequency domains to justify the model accuracy for effective controller design.

3. RESULTS AND DISCUSSION

3.1. Performance of the PS-FB DC-DC Converter

The PS-FB DC-DC ZVS converter performance was investigated for different loading conditions. The results for soft switching range focusing on both full load conditions, are provided as follows: the ZVS PS-FB DC-DC converter simulation results including transformer primary and secondary voltage-current waveform, are presented in Fig. 3(a) and 3(b). In Fig. 3(a), the H-bridge inverter voltage switches between V_{dc} (48V) and $-V_{dc}$ (-48V) and the primary current (I_p) (red) flow in a positive direction to reach the reflected inductor

output current (nL_o) when diagonal switches S_1 and S_4 are in the *on*-state condition. Also, the current flow in a negative direction when the diagonal switches S_2 and S_3 are in *on*-state completing a full switching cycle.

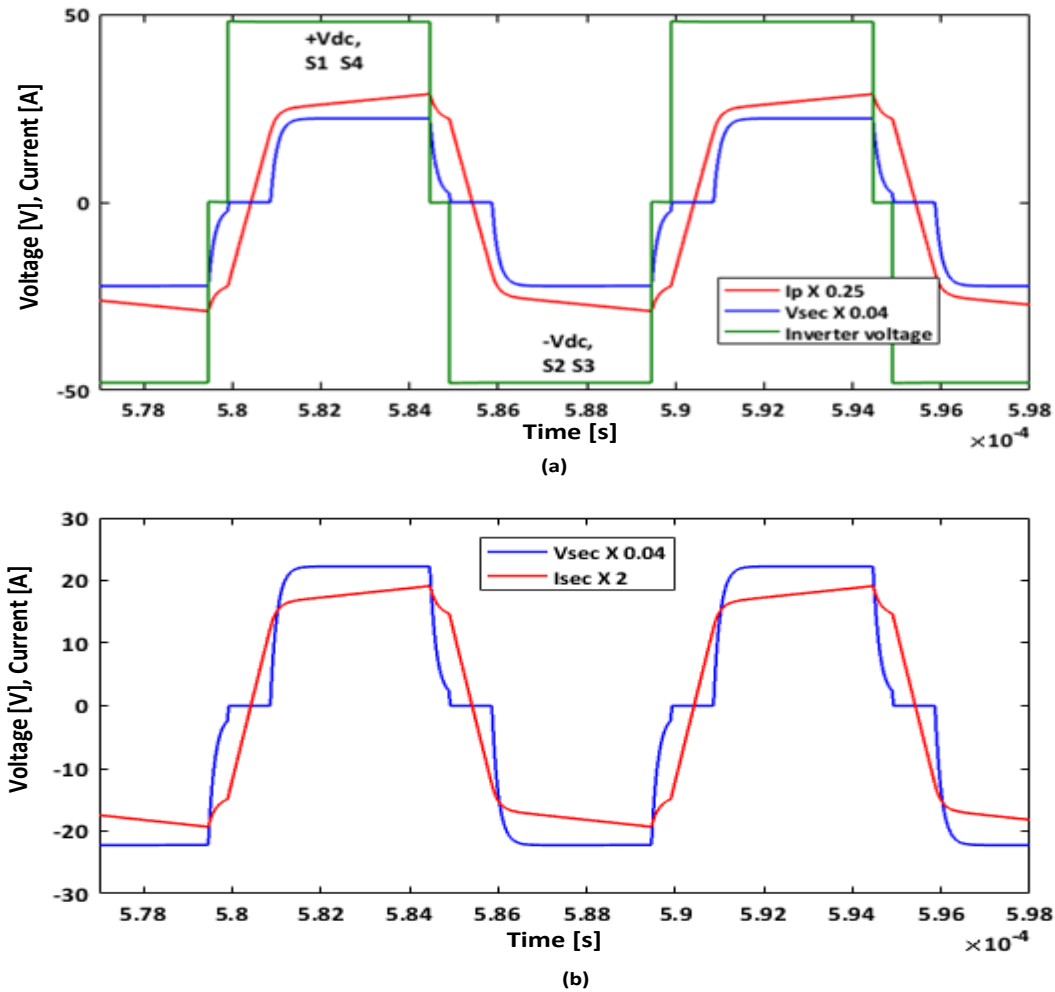


Fig. 3. Transformer's voltage-current waveforms: a) primary voltage-current waveform; b) secondary voltage-current waveform.

The output inductor current ripple is designed for 1.5 A for continuous conduction operation and this can be observed from the load current waveform presented in Fig. 4 with an average peak value of about 7.5 A as expected under full rated load.

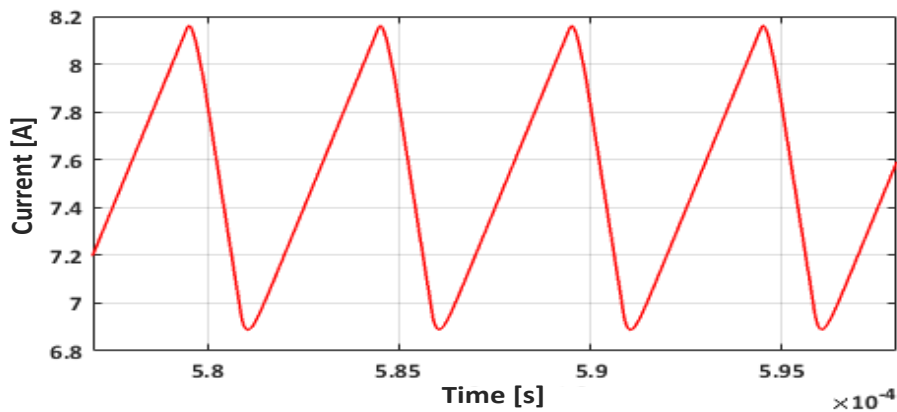


Fig. 4. Load current waveform.

The voltage and current switching waveforms for both leading leg switch S_2 and lagging leg S_4 of the H-inverter are presented in Fig. 5(a) and (b). Fig. 5 (a), as well as Fig. 5 (b), show that the drain-source voltage (V_{DS}) is at zero before the gate-source voltage (V_{GS}) starts rising confirming the zero-voltage switching condition during the turn-on transition of MOSFET. When the snubber capacitance (C_{GS}) is completely discharged from V_{DS} to 0 V, the MOSFET body diode starts to conduct and put it in *on*-state with zero voltage switching transition, and this drastically reduces the switching losses. Both MOSFET switches S_2 and S_4 waveform from each leg show that the MOSFET conveniently achieved ZVS.

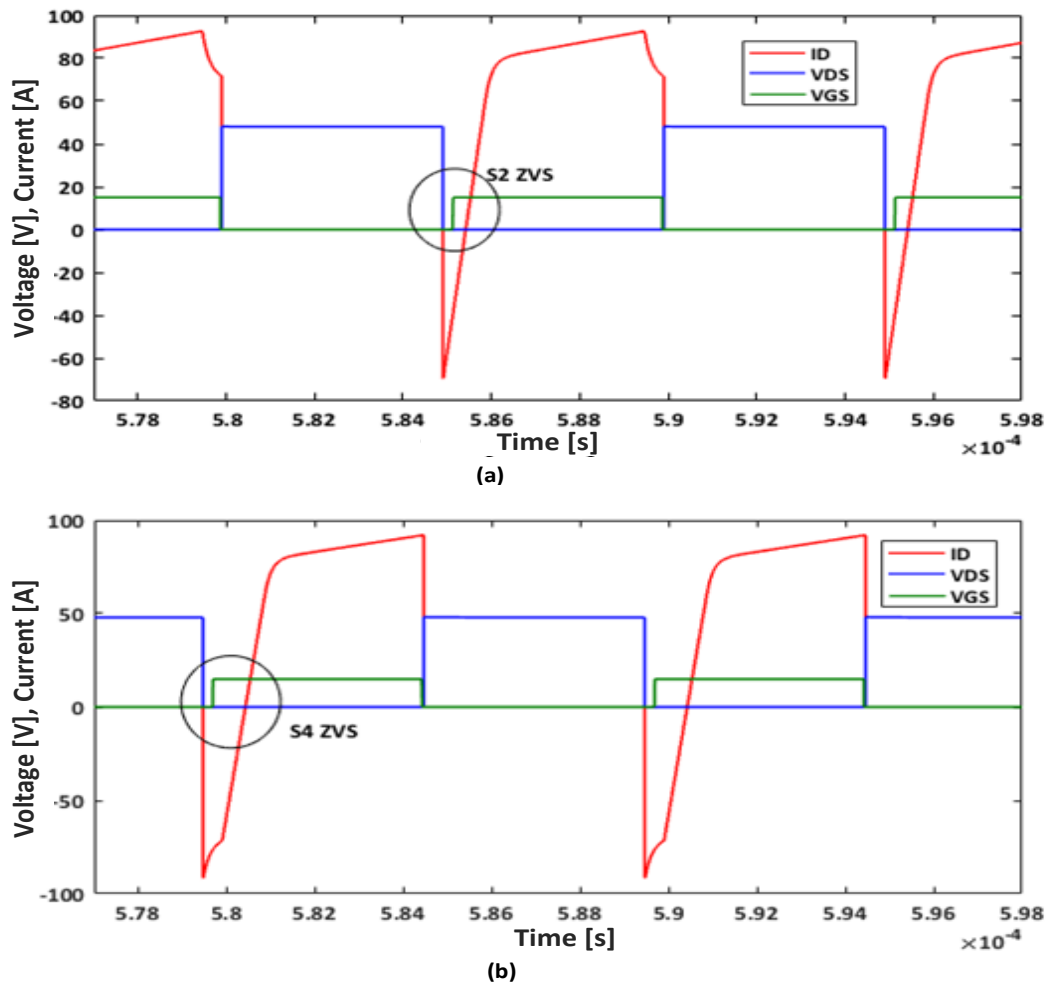


Fig. 5. Switching waveform for: a) leading leg switch S_2 ; b) lagging leg switch S_4 .

3.2. Converter Input-Output Voltage Response

Test measurements were conducted on the converter to obtain the input-output voltage data using the same sampling frequency as the simulation step-time. The converter voltage measurement data sets - that include the model data and two validation data - are plotted in Figs. 6-8 respectively. The converter model data presented in Fig. 6 is used for estimating the converter model parameters for 4 different model structures appearing in Table 2.

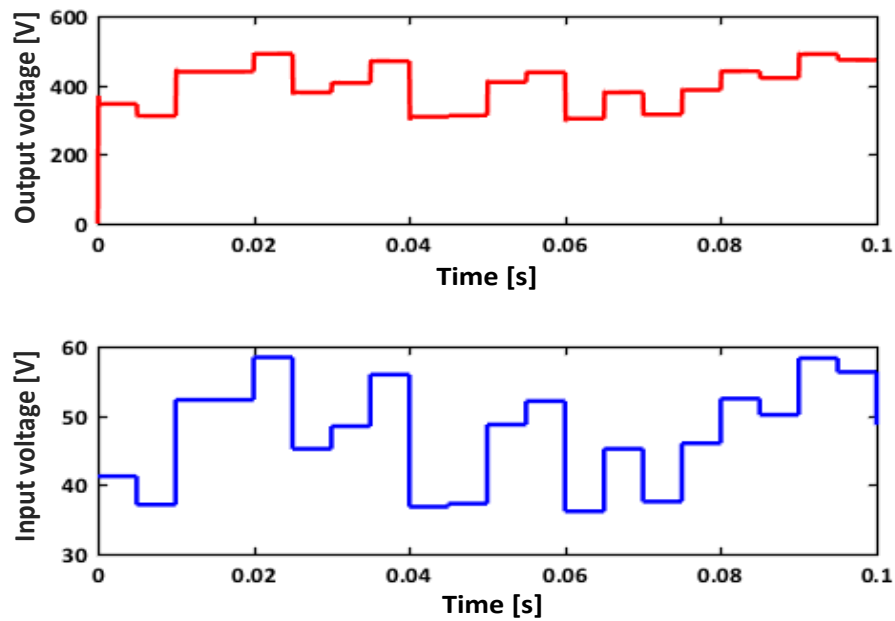


Fig. 6. Converter input-output voltage - model data.

Table 2. Converter identified parameters.

Parameters	Estimated value tf1	Estimated value tf2	Estimated value tf3	Estimated value tf4
a_1	5534	$1.497e^4$	8593	$1.537e^4$
a_2	-	$8.854e^7$	$4.393e^7$	$9.02e^7$
a_3	-	-	-	$1.407e^{10}$
b_o	-	-	$1.283e^4$	$7.39e^8$
b_1	$4.663e^4$	$7.458e^8$	$3.697e^8$	$1.186e^{11}$

To ascertain the accuracy and robustness of the DC-DC converter dynamic model structure, the other two independent validation test data shown in Figs. 7 and 8 were used for the model validation.

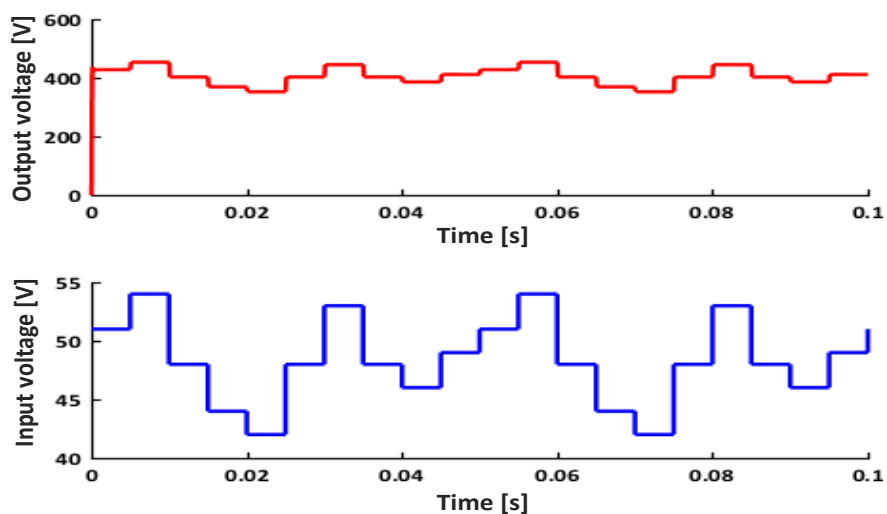


Fig. 7. Converter validation data 1.

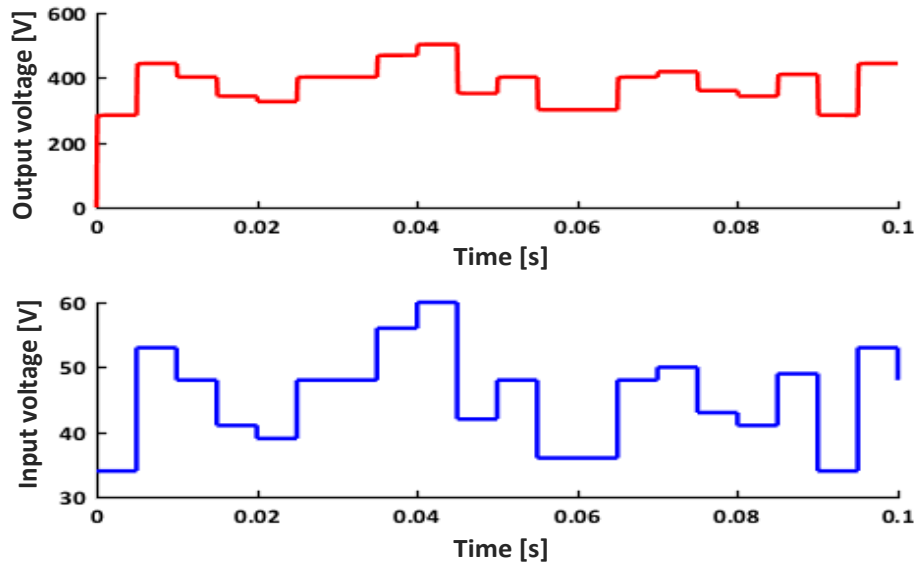


Fig. 8. Converter validation data 2.

3.3. Estimated Converter Model Parameters

The DC-DC converters generally exhibit nonlinear behaviour due to the dynamic nature of basic element which is the switches. Switching devices such as MOSFET have parasitic capacitance that affects their behaviour and limits their operating frequency. This effect requires the converter model to be very accurate to capture this phenomenon to aid any effective model-based controller design. In this study, a system identification approach has been used to model the PS-FB ZVS converter and the model parameters are presented in this subsection. Four model structures were selected to obtain the converter transfer function and the estimated parameters for each of the selected structure is presented in Table 2. The model structure has a varying number of Zeros and Poles assigned **tf1**, **tf2**, **tf3**, and **tf4**. Also, Table 3 presents the control-to-output transfer function (G_{vd}) of the DC-DC converter as obtained from the system identification approach with the summary of percentage fit when tested with the validation data.

Table 3. Transfer function and model fit for the selected mode structures.

	Transfer function	Model [%]	Val-1 fit [%]	Val-2 fit [%]
tf1	$\frac{4.663e^4}{s + 5534}$	96.57	92.98	95.67
tf2	$\frac{7.458e^8}{s^2 + 1.497e^4s + 8.854e^7}$	98.55	94.29	96.02
tf3	$\frac{1.283e^4s + 3.697e^8}{s^2 + 8593s + 4.393e^7}$	99	95.65	96.36
tf4	$\frac{7.39e^8s + 1.186e^{11}}{s^3 + 1.537e^4s^2 + 9.02e^7s + 1.407e^{10}}$	98.56	94.72	96.22

The **tf1** is a first-order model with 1-pole and has a model fit of 96.56%. The second selected structure **tf2** is a second-order model with 2-poles and no zero having a 98.55% model fit as presented in Table 3. The **tf3** is also a second order system of 2-poles and 1-zero to cater for the output capacitor zero and the model has 99% fit. The **tf4** is a third-order function with 3-poles and 1-zero used as a test to verify if higher-order will provide a better model fit for the system. It was found that the model fit is 98.56% which is slightly lower than 99% fit obtained for **tf3**.

The second-order model **tf3** with 2-poles, 1-zeros has the best model fit and was able to repeat the system behaviour with 95.65% and 96.36% fits when tested with independent validation data-1 and data-2 respectively. This was higher than the model fit returned by remaining model structures, with the next highest value of 94.72% for validation test data-1 and 96.22% for validation data-2 obtained from **tf4**. The second-order model **tf3** having highest model fit with test data shows that most of the complex and nonlinear system such as PWM switching converter can be modelled as a second order system. The transfer function for all the model structure presented in Table 3, column 2 shows that all the systems poles are on the left-hand plan confirming that the Simulink model converter is stable under open-loop operation.

The selected model structure **tf1**, **tf2**, **tf3**, and **tf4** were further analysed in the frequency domain to confirm their stability and correlation with the mathematical model recently published in [12]. As observed in the model frequency response plotted in Fig. 9(a), the **tf3** bode plot has an infinite gain and 60.6° phase margin at 3.44 kHz crossover frequency showing good stability. The **tf3** frequency response is similar to the enhanced model of ZVS PS-FB DC-DC converter recently proposed by Di Capua et al. [12] and this confirms the accuracy of the obtained converter model. Particularly, there is good agreement between the frequency response of the converter model obtained using identification modelling approach and that of the enhanced mathematical dynamic model presented by Di Capua et al. [12] as presented in Fig. 9.

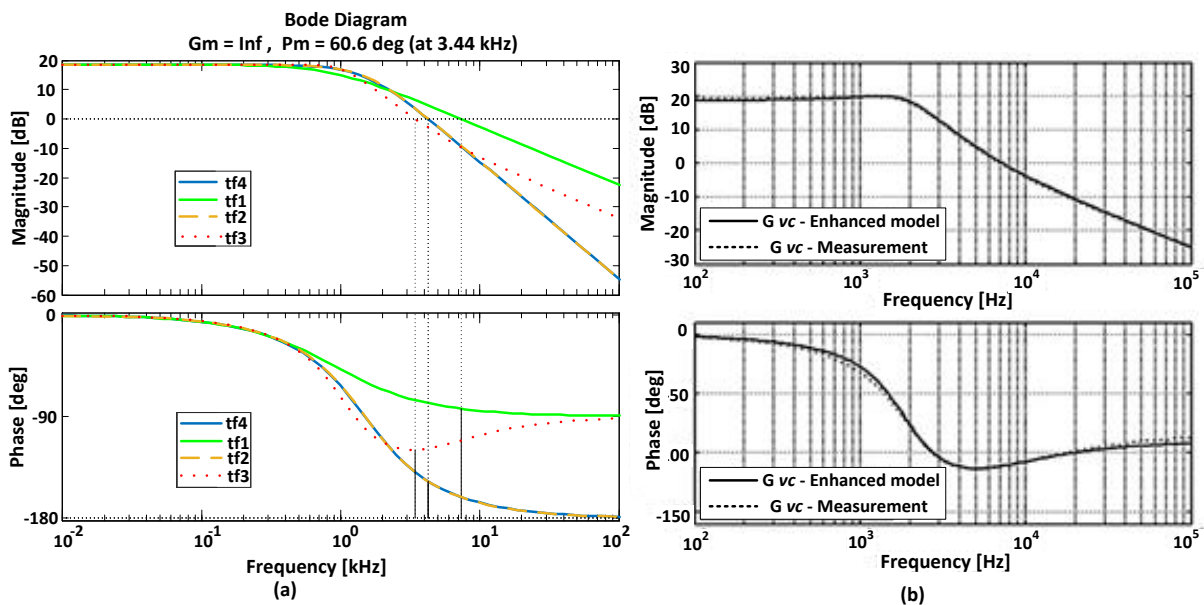


Fig. 9. a) Obtained converter control-to-output transfer function (**tf3**); b) measured control-to-output transfer function [6].

4. CONCLUSIONS

A system identification approach was proposed for obtaining an accurate model of phase-shifted full-bridge ZVS DC-DC converter. The approach provided an alternative to the rigorous and complex mathematics involve when using first principle approach if all switching transitional stages of the converter are to be considered. The circuit parasitic that plays a key role in the system dynamic performance was given adequate consideration using system identification method which resulted in a more accurate model for effective controller design to deliver tight output voltage regulation. Comparing the model frequency response with other published mathematical and measured values confirmed the model accuracy and suitability. The result also shows that higher-order model does not necessarily represent the best system dynamic fit of a system as observed between second-order **tf3** which produced a slightly better model fit on the validation data compared to third-order **tf4**.

REFERENCES

- [1] A. Ghosh, S. Banerjee, "Control of switched-mode boost converter by using classical and optimized type controllers," *Journal of Control Engineering and Applied Informatics*, vol. 17, no. 4, pp. 114-125, 2015.
- [2] C. Tse, M. Di Bernardo, "Complex behavior in switching power converters," *Proceedings of the IEEE*, vol. 90, no. 5, pp. 768-781, 2002.
- [3] Z. Cui, N. Cui, C. Wang, C. Li, C. Zhang, "A robust online parameter identification method for lithium-ion battery model under asynchronous sampling and noise interference," *IEEE Transactions on Industrial Electronics*, 2020.
- [4] M. Elshimy, M. Abd El Ghany, D. Göhringer, "SysIDLib: a high-level synthesis FPGA library for online system identification," *Proceedings of Applied Reconfigurable Computing. Architectures, Tools, and Applications: 16th International Symposium*, Toledo, Spain, pp. 97-107, 2020.
- [5] M. Simoiu, V. Calofir, S. Iliescu, I. Fagarasan, N. Arghira, "BOOST converter modelling as a subsystem of a photovoltaic panel control system," *2020 IEEE International Conference on Automation, Quality and Testing, Robotics*, pp. 1-6, 2020.
- [6] G. Nobile, E. Vasta, M. Cacciato, G. Scarcella, G. Scelba, A. Di Stefano, G. Leotta, P. Pugliatti, F. Bizzarri, "Performance assessment of large photovoltaic (PV) plants using an integrated state-space average modeling approach," *Energies*, vol. 13, no. 18, p. 4777, 2020.
- [7] S. Ang, A. Oliva, *Power-Switching Converters*, CRC Press, 2005.
- [8] N. Trip, S. Lungu, V. Popescu, "Modelling of switched mode fly-back supply for engineering education," *Advances in Electrical and Computer Engineering*, vol. 10, no. 1, pp. 100-105, 2010.
- [9] L. Huang, Y. Zhou, J. Huang, J. Zeng, G. Chen, "Analysis and design of ZVZCS full-bridge converter with reduced components for input-series-output-parallel application," *IEEE Transactions on Industrial Electronics*, 2020.
- [10] V. Kumar, R. Behera, D. Joshi, R. Bansal, *Power Electronics, Drives, and Advanced Applications*, CRC Press, 2020.
- [11] V. Vlatkovic, J. Sabate, R. Ridley, F. Lee, B. Cho, "Small-signal analysis of the phase-shifted PWM converter," *IEEE Transactions on Power Electronics*, vol. 7, no. 1, pp. 128-135, 1992.
- [12] G. Di Capua, S. Shirsavar, M. Hallworth, N. Femia, "An enhanced model for small-signal analysis of the phase-shifted full-bridge converter," *IEEE Transactions on Power Electronics*, vol. 30, no. 3, pp. 1567-1576, 2015.

- [13] F. Tsai, "Small-signal and transient analysis of a zero-voltage-switched, phase-controlled PWM converter using averaged switch model," *IEEE Transactions on Industry Applications*, vol. 29, no. 3, pp. 493-499, 1993.
- [14] V. Vorpérian, "Simplified analysis of PWM converters using model of PWM switch. II. Discontinuous conduction mode," *IEEE Transactions on Aerospace and Electronic Systems*, vol. 26, no. 3, pp. 497-505, 1990.
- [15] M. Schutten, D. Torrey, "Improved small-signal analysis for the phase-shifted PWM power converter," *IEEE Transactions on Power Electronics*, vol. 18, no. 2, pp. 659-669, 2003.
- [16] L. Yu, S. Xu, H. Zhang, L. Shi, W. Sun, "An auto-tuning method based on system identification for digitally controlled synchronous buck converter," *IEEE Journal of Emerging and Selected Topics in Power Electronics*, 2020.
- [17] M. Badoni, A. Singh, B. Singh, "Comparative performance of wiener filter and adaptive least mean square-based control for power quality improvement," *IEEE Transactions on Industrial Electronics*, vol. 63, no. 5, pp. 3028-3037, 2016.
- [18] O. Oyerinde, "Reweighted regularised variable step size normalised least mean square-based iterative channel estimation for multicarrier-interleave division multiple access systems," *IET Signal Processing*, vol. 10, no. 8, pp. 947-954, 2016.
- [19] M. Beza, M. Bongiorno, "Application of recursive least squares algorithm with variable forgetting factor for frequency component estimation in a generic input signal," *IEEE Transactions on Industry Applications*, vol. 50, no. 2, pp. 1168-1176, 2014.
- [20] R. Arablouei, K. ı l Dogancay, "Reduced-complexity constrained recursive least-squares adaptive filtering algorithm," *IEEE Transactions on Signal Processing*, vol. 60, no. 12, pp. 6687-6692, 2012.
- [21] P. Regulski, D. Vilchis-Rodriguez, S. Djurović, V. Terzija, "Estimation of composite load model parameters using an improved particle swarm optimization method," *IEEE Transactions on Power Delivery*, vol. 30, no. 2, pp. 553-560, 2015.
- [22] M. Badoni, A. Singh, B. Singh, "Variable forgetting factor recursive least square control algorithm for DSTATCOM," *IEEE Transactions on Power Delivery*, vol. 30, no. 5, pp. 2353-2361, 2015.
- [23] M. Ahmeid, M. Armstrong, S. Gadoue, M. Al-Greer, P. Missailidis, "Real-time parameter estimation of DC-DC converters using a self-tuned kalman filter," *IEEE Transactions on Power Electronics*, vol. 30, no. 7, pp. 5666-5674, 2016.
- [24] A. Hajizadeh, A. Shahirinia, N. Namjoo, C. David, "Self-tuning indirect adaptive control of non-inverting buck-boost converter," *IET Power Electronics*, vol. 8, no. 11, pp. 2299-2306, 2015.
- [25] J. Li, Y. Zheng, Z. Lin, "Recursive identification of time-varying systems: Self-tuning and matrix RLS algorithms," *Systems and Control Letters*, vol. 66, pp. 104-110, 2014.
- [26] M. Al-Greer, M. Armstrong, D. Giaouris, "Adaptive PD+ I control of a switch-mode DC-DC power converter using a recursive FIR predictor," *IEEE Transactions on Industry Applications*, vol. 47, pp. 2135-2144, 2011.
- [27] V. Mathews, *Circuits and Systems Tutorials: Adaptive Polynomial Filters*, IEEE Press, pp. 59-64, 1996.
- [28] B. Lin, K. Huang, D. Wang, "Analysis and implementation of full-bridge converter with current doubler rectifier," *IEE Proceedings-Electric Power Applications*, vol. 152, no. 5, pp. 1193-1202, 2005.
- [29] O. Ibrahim, N. Yahaya, N. Saad, K. Ahmed, "Design and simulation of phase-shifted full bridge converter for hybrid energy systems," *2016 6th International Conference on Intelligent and Advanced Systems*, pp. 1-6, 2016.
- [30] L. Ljung, *System Identification - Theory for the User*, PTR Prentice Hall, 1999.
- [31] A. Tangirala, *Principles of System Identification: Theory and Practice*, CRC Press, 2014.